Molecular Therapy
Original Article

Modifying Antigen-Encapsulating Liposomes with KALA Facilitates MHC Class I Antigen Presentation and Enhances Anti-tumor Effects

Naoya Miura,[1,3] Hidetaka Akita,[2,3] Naho Tateshita,[2] Takashi Nakamura,[1] and Hideyoshi Harashima[1]

[1]Department of Molecular Design of Pharmaceutics, Faculty of Pharmaceutical Sciences, Hokkaido University, Kita 12, Nishi 6, Kita-ku, Sapporo City, Hokkaido 060-0812, Japan; [2]Laboratory of Pharmacology and Toxicology, Graduate School of Pharmaceutical Sciences, Chiba University, 1-8-1 Inohana, Chuo-ku, Chiba City, Chiba 263-8675, Japan

For a successful anti-cancer vaccine, antigen presentation on the major histocompatibility complex (MHC) class I is a requirement. To accomplish this, an antigen must be delivered to the cytoplasm by overcoming the endosome/lysosome. We previously reported that a lipid nanoparticle modified with a KALA peptide (WEAKLAKALAKALAKHLAKALAKALKA), an α-helical cationic peptide, permits the encapsulated pDNA to be efficiently delivered to the cytoplasm in bone marrow-derived dendritic cells (BMDCs). Herein, we report on the use of KALA-modified liposomes as an antigen carrier, in an attempt to induce potent antigen-specific cellular immunity. The subcutaneous injection of KALA-modified ovalbumin (OVA)-encapsulating liposomes (KALA-OVA-LPs) elicited a much more potent OVA-specific cytotoxic T lymphocyte activity and anti-tumor effect in comparison with particles that were modified with octa-arginine (R8), a cell-penetrating peptide (R8-OVA-LPs). In addition, the numbers of OVA-specific $CD8^+$ T cells were increased by immunization the KALA-OVA-LPs. The treatment of BMDCs with KALA-OVA-LPs induced a substantial MHC class I antigen presentation. Furthermore, the acidic pH-dependent membrane destabilization activity of KALA-OVA-LPs strongly suggests that they are able to escape from endosomes/lysosomes and thereby deliver their cargos to the cytoplasm. Collectively, the KALA-modified liposome is a potential antigen delivery platform for use as a protein vaccine.

INTRODUCTION

Antigen presentation on the major histocompatibility complex (MHC) class I in antigen-presenting cells (APCs) (e.g., dendritic cells [DCs], macrophages) is particularly important for the induction of cellular immunity, an immunological action that plays a key role in effective cancer immunotherapy via the activation of antigen-specific cytotoxic T lymphocytes (CTL).[1–5] An exogenous antigen is usually degraded into peptide fragments in endosome/lysosomes and presented in the context of MHC class II, thereby activating $CD4^+$ T cells to induce humoral immunity. Therefore, a strategy for delivering the antigen to the cytoplasm is prerequisite for the effective activation of cellular immunity, because the antigen must be subjected to proteasomal degradation for antigen presentation onto the MHC class I ("cross-presentation").

To accomplish efficient antigen delivery, considerable efforts have been devoted to developing various drug delivery carriers.[6–8] The liposome is one of the most useful carriers for antigens because they contain an inner aqueous phase in which water-soluble molecules can be encapsulated.[9–11] Furthermore, when the surfaces of liposomes are modified with functional molecules (i.e., peptides, carbohydrates, and antibodies), this can facilitate the efficient delivery of an antigen.[6,10,12–15] For efficient cellular uptake, the use of cationic liposomes (i.e., N-[1-(2,3-dioleoyloxy)propyl]-N, N, N-trimethylammonium methyl-sulfate [DOTAP]) can be beneficial, because it can be inherently absorbed on the cellular surface. Moreover, it is well known that cationic nanoparticles are taken up by macrophages in vitro and in vivo (i.e., Kupffer cells).[16,17] We previously reported on the development of a liposome-based antigen carrier, octa-arginine (R8)-modified liposomes.[18] Modification with R8, which mimics the TAT peptide of the influenza virus, enhanced endosomal escape, as well as the uptake of the liposomes in murine bone marrow-derived dendritic cells (BMDCs), compared with simple cationic liposomes. Furthermore, the R8-modified liposomes that contained encapsulated ovalbumin (OVA) elicited efficient antigen presentation in the context of MHC class I and an OVA-specific anti-tumor effect, while conventional DOTAP liposomes preferred MHC class II-mediated antigen presentation. Thus, the rational design of functional molecules for delivering an antigen to the cytoplasm allowed us to develop an effective anti-tumor vaccine system.

Received 2 June 2016; accepted 23 January 2017;
http://dx.doi.org/10.1016/j.ymthe.2017.01.020.

[3]These authors contributed equally to this work

Correspondence: Hidetaka Akita, Laboratory of Pharmacology and Toxicology, Graduate School of Pharmaceutical Sciences, Chiba University, 1-8-1 Inohana, Chuo-ku, Chiba City, Chiba 263-8675, Japan.
E-mail: akitahide@chiba-u.jp
Correspondence: Hideyoshi Harashima, Department of Molecular Design of Pharmaceutics, Faculty of Pharmaceutical Sciences, Hokkaido University, Kita 12, Nishi 6, Kita-ku, Sapporo City, Hokkaido 060-0812, Japan.
E-mail: harasima@pharm.hokudai.ac.jp

Table 1. Physicochemical Properties of the Various OVA-LPs

Liposome	Size (nm)	ζ Potential (mV)
OVA-Lp (DOPE)	158 ± 2	−19 ± 1
OVA-Lp (EPC)	162 ± 1	−37 ± 11
KALA-OVA-Lp (DOPE)	169 ± 4	50 ± 1
KALA-OVA-Lp (EPC)	185 ± 32	30 ± 1
R8-OVA-Lp (DOPE)	178 ± 4	52 ± 1
R8-OVA-Lp (EPC)	169 ± 2	52 ± 4

Data are represented as mean ± SEM of at least three independent experiments (n = 3–15).

We recently reported on the development of a KALA-modified lipid nanoparticle containing pDNA (a multi-functional envelope-type nano device [KALA-MEND]) as a carrier of a DNA vaccine.[19,20] The key component (KALA) in this system adopts an α-helical structure at physiological pH for membrane destabilization.[21] To modify the liposomal structure with it, the peptide was stearylated. As a result, the KALA-MEND exhibited >2 orders of magnitude higher gene transfection activity in comparison with the R8-modified one (R8-MEND) in BMDCs. Moreover, it unexpectedly induced the production of a large variety of cytokines and chemokines via the stimulation of cytosolic DNA sensors (i.e., TBK1/STING pathway, AIM-2 inflammasome). These results indicate that KALA-modified liposomes are more beneficial for delivering encapsulating cargos to the cytoplasm in comparison with R8-modified particles. This observation prompted us to evaluate the possibility of using the KALA peptide to deliver an antigen protein to cells for a cancer vaccine. The focus of this study was on the induction of the antigen presentation on MHC class I molecules and the resulting cellular immunity for cancer therapeutics.

RESULTS

Measurement of OVA-Specific CTL Activity in Mice Immunized with KALA-OVA-LPs

To evaluate the efficiency of the KALA peptide for antigen protein delivery, we designed KALA peptide-modified OVA-encapsulating liposomes (KALA-OVA-LPs). The liposomes were composed of three types of lipids: 1,2-dioleoyl sn-glycero-3-phosphoethanolamine (DOPE) (a membrane-fusogenic lipid for overcoming the biomembrane barrier), cholesteryl hemisuccinate (CHEMS) (a pH-sensitive lipid for creating sensitivity to a low-pH environment; endosomes/lysosomes), and egg phosphatidylcholine (EPC) (a membrane-stabilizing lipid for the formation of liposomes), as reported previously.[18] To increase the membrane-fusogenic activity of the liposomes, DOPE was used in the lipid composition, while an EPC-based particle was used as a non-fusogenic control, in order to clarify the relationship between membrane-fusogenic property and vaccine activity. The OVA protein was encapsulated in liposomes by repetitive freeze and thaw cycles. After liposomal formation, the surfaces of the liposomes were modified with the KALA peptide by adding a lipid derivative of the KALA peptide (STR-KALA). As a control for the cationic peptide, octa-arginine (R8) was used to modify the particles, instead of KALA (R8-OVA-LPs). The physicochemical properties of each liposome preparation are shown in Table 1. The modification with STR-KALA or STR-R8 resulted in a large increase in ζ potential (to approximately +50 mV), while the size and polydispersity index (PdI) were comparable with the values for non-modified OVA-LPs (approximately 160–170 nm and 0.15, respectively).

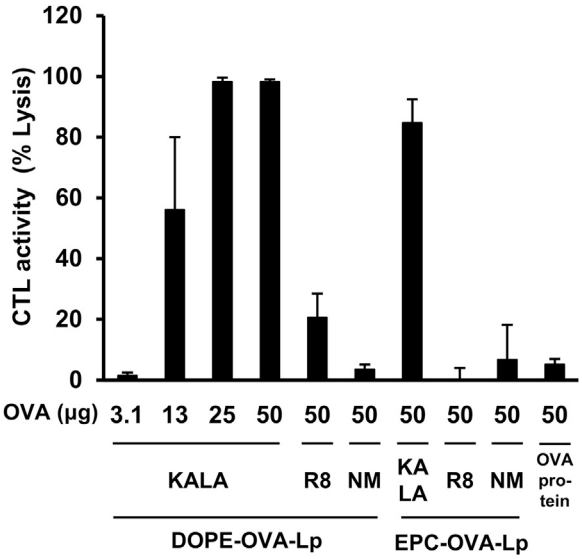

Figure 1. In Vivo CTL Assay

C57BL/6 mice were immunized subcutaneously once with KALA-OVA-LPs, R8-OVA-LPs, OVA-LPs (DOPE or EPC as a helper lipid), or free OVA protein at a dose of 3.1, 13, 25 (KALA-OVA-LPs only), or 50 μg OVA. Fluorescent-labeled target cells ($OVA_{257–264}$ pulsed, $CFSE^{High}$) and control cells (no peptide pulsed, $CFSE^{Low}$) were injected intravenously at 1 week after immunization. The OVA-specific lysis was calculated from the target cell/control cell ratio measured by flow cytometer 20 hr after injection. Data are mean + SEM (n = 3–5).

In initial experiments, we evaluated the impact of the modification of the KALA peptide on the induction of antigen-specific cellular immunity in vivo. To investigate this, in vivo OVA-specific CTL activity was evaluated after subcutaneous immunization of the KALA-OVA-LPs. The liposomes containing the indicated amount of OVA, free OVA, or empty KALA-modified liposomes (KALA-LPs) were subcutaneously injected into the back of the necks of the mice one time. OVA-specific CTL activity was evaluated 7 days after immunization (Figure 1). First, immunization with the OVA protein per se did not induce CTL activity. In contrast, a dose-dependent increase in CTL activity was achieved when the OVA was immunized using the DOPE-incorporated KALA-OVA-LPs, whereas the CTL activity for the R8-OVA-LPs was marginal, even in the case of a maximum dose (50 μg). Of note, the corresponding activities for non-modified OVA-LPs were at the background level. These data collectively indicate that KALA is a key component for the effective induction of CTL activity. Although the EPC-incorporated KALA-OVA-LPs also induced significant CTL activity, the activity was inferior to that for the DOPE-based KALA-OVA-LPs, suggesting that modification

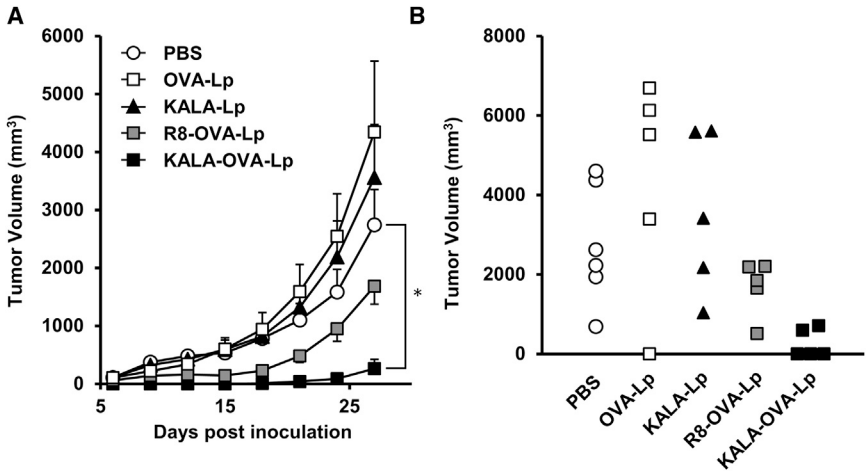

Figure 2. Anti-tumor Effect of OVA-Encapsulating Liposomes

(A) C57BL/6 mice were immunized subcutaneously once with KALA-OVA-LPs, R8-OVA-LPs, OVA-LPs, or KALA-LPs at a dose of 25 μg OVA. For the injection of KALA-LPs (empty liposomes), the dose of the lipid was adjusted to that for the KALA-OVA-LPs. One week after immunization, mice were inoculated with 8.0×10^5 cells of E.G7-OVA in the left flank. The tumor volume was measured up to 27 days after inoculation. The plots represent the mean ± SEM (n = 5–6). Statistical analyses were performed using one-way ANOVA, followed by the Bonferroni test. *$p < 0.05$ versus PBS group. (B) The tumor volumes in individual mice on day 27 were plotted.

with the fusogenic lipid envelope and KALA synergistically potentiated the immune stimulative activity.[20] Furthermore, the KALA-OVA-LPs induced significant CTL activity by single immunization at a dose of 13 μg OVA, a smaller dose in comparison with previous studies.[22,23] Collectively, these data suggest that the DOPE-based KALA-OVA-LPs have the potential for use as an anti-cancer vaccine system.

Anti-tumor Effect of KALA-OVA-LPs

To prove the potential of KALA-OVA-LPs as an anti-cancer vaccine, the prophylactic anti-tumor effect against E.G7-OVA, a mouse lymphoma EL4 expressing the OVA gene, was evaluated. Mice were immunized with KALA-OVA-LPs, R8-OVA-LPs, non-modified OVA-LPs (equivalent to 25 μg of OVA) or empty KALA-LPs (the same amount of lipid as KALA-OVA-LPs) subcutaneously one time. The immunized mice were inoculated with E.G7-OVA in the right flank 1 week after immunization. Tumor volume was then monitored for up to 27 days after tumor inoculation (Figure 2A). The immunization by the non-modified OVA-LPs failed to inhibit tumor growth, suggesting that the induction of OVA-specific immunity was insufficient. Consistent with data from a previous study, immunization with the R8-OVA-LPs inhibited tumor growth, although the effect was marginal at this dose. On the other hand, immunization with the KALA-OVA-LPs exhibited a significant anti-tumor effect: tumor growth was completely suppressed up to day 15, and furthermore, in three of five mice, tumor growth was not detectable, even on day 27 (Figure 2B). Consequently, antigen-encapsulating KALA-modified liposomes were more potent as an anti-cancer vaccine in comparison with the R8-modified particles.

To demonstrate the anti-tumor effect of the KALA-OVA-LPs in a more representative clinical setting, therapeutic anti-tumor experiments were carried out. Mice were inoculated with E.G7-OVA cells, followed by immunization with the KALA-OVA-LPs. Furthermore, to evaluate the synergistic effect of an immune checkpoint inhibitor on the therapeutic effect, mice were treated with an anti-PD-1 antibody when they were immunized with KALA-OVA-LPs. As a result, tumor volume tended to decrease on average as the result of immunization with the KALA-OVA-LPs (Figure S1A). Because the tumor volume of vehicle control animals was largely varied (tumor rejection occurred on day 20 in only one of five mice), no significant differences were observed. However, the administration of the KALA-OVA-LPs suppressed the tumor growth in four of five mice (less than 500 mm^3 on day 20), whereas only two of five mice were found to be less than 500 mm^3 on day 20 in the vehicle treatment group (Figure S1B). Furthermore, whereas anti-PD-1 antibody-treated group reached an average of 1,000 mm^3 on day 20, the group that had the combined KALA-OVA-LPs and anti-PD-1 treatment decreased on average by half (Figure S1A). These results suggest that KALA-OVA-LPs are potent in anti-tumor vaccines in a clinical setting and that they enhance the action of immune checkpoint inhibitors.

MHC Class I Antigen Presentation by KALA-OVA-LPs

To elucidate the mechanism responsible for the more prominent induction of in vivo OVA-specific immunity, we evaluated the antigen presentation activity of the KALA-OVA-LPs in vitro. In this analysis, BMDCs were used, as it is well known that DCs have a crucial role in the induction of antigen-specific immunity.[24,25] We first evaluated the innate immune activation of BMDCs in terms of enhancing the activation of CD80/86, markers of immune stimulation in BMDCs. However, no activation was observed even when KALA-OVA-LPs were administered (Figure S2). This is consistent with the fact that an inflammatory immune response (IL-6 production in serum) was not observed after the injection of the KALA-OVA-LPs (Figure S3). We then investigated a OVA-specific antigen presentation on MHC class I. Antigen presentation was quantified by co-cultivation with B3Z T cell hybridoma, a reporter cell line that produces the lacZ protein in response to the $OVA_{257–264}$ epitope bound to $H\text{-}2K^b$.[26] As a result, modification with STR-KALA drastically enhanced antigen presentation from BMDCs, depending on the amount of modification (Figure 3A). The effect of KALA modification approached saturation at 5 mol% of total lipids, whereas almost no antigen presentation was

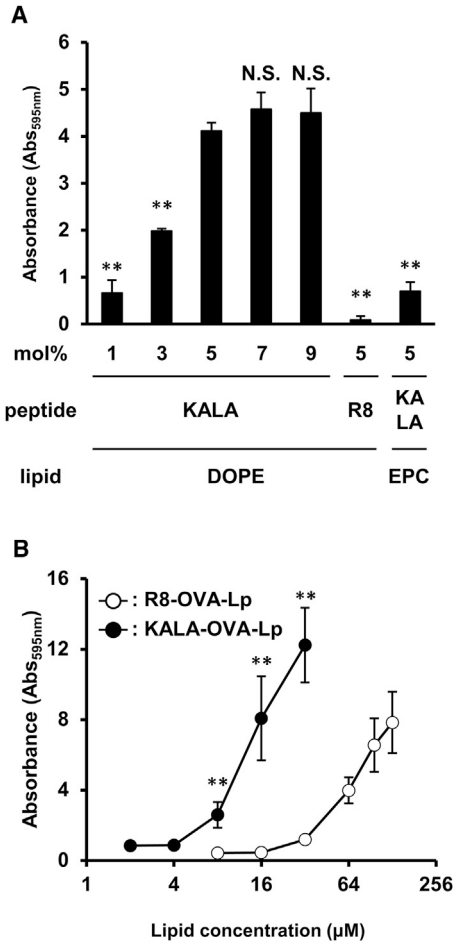

Figure 3. Evaluation of MHC Class I Antigen Presentation

(A) BMDCs were treated with several types of KALA-OVA-LPs (DOPE or EPC as a helper lipid), modified with the KALA peptide (1, 3, 5, 7, or 9 mol% of total lipid) or R8-OVA-LPs (DOPE as a helper lipid, modified with R8 peptide (5 mol% of total lipid) at a dose of 10 μM of lipid. After 5 hr, the treated cells were co-cultured with a B3Z T cell hybridoma, specific for the $OVA_{257–264}$ epitope in the context of $K^{b,\,41}$ for 15 hr at 37°C. The co-cultured cells were lysed and incubated with chrolophenol red β-D-galactopyranoside buffer for 4 hr at 37°C. The absorbance at 595 nm was used as an index for antigen presentation activity. Data are mean + SD (n = 3). Statistical analyses were performed using one-way ANOVA, followed by the Dunnett test. **p < 0.01 versus 5 mol% KALA-OVA-LPs composed of DOPE. N.S., not significant. (B) BMDCs were treated with the KALA-OVA-LPs or R8-OVA-LPs at several doses. Data are mean ± SD (n = 3). Statistical analyses were performed using Student's t test. **p < 0.01.

observed in R8-OVA-LPs treatment at the corresponding density. Comparing the dose-response curves, the antigen presentation efficiency of the KALA-OVA-LPs at a dose of 16 μM approached those of R8-OVA-LPs at a dose of 128 μM, suggesting that KALA modification resulted in an enhancement in antigen presentation activity that was 8 times higher than that for R8 modification (Figure 3B). The BMDCs treated with KALA-OVA-LPs elicited anti-tumor effects against E.G7-OVA when they were immunized via the footpad. This suggests that the enhanced antigen presentation in DCs is one of the mechanisms responsible for the anti-tumor activity of KALA-OVA-LPs (Figure S4). Furthermore, the enhancement of antigen presentation by modification with KALA was reduced when the lipid was replaced from DOPE to the non-fusogenic EPC (Figure 3A). This result is consistent with the results of in vivo CTL assays. It appears that the KALA peptide is a potent activator for a liposomal antigen delivery system for the achievement of antigen presentation to MHC class I.

In Vitro and In Vivo Cellular Uptake and Membrane-Fusogenic Activity of the KALA-OVA-LPs

To gain further insights into the mechanism underlying the difference in immunological action between KALA-OVA-LPs and R8-OVA-LPs, in vitro and in vivo cellular uptake and membrane-fusogenic activity were evaluated. The kinetics of the ex vivo cellular uptake of KALA-OVA-LPs and R8-OVA-LPs using BMDCs were first compared by means of flow cytometry. Liposomes encapsulating a fluorescence-labeled OVA (Alexa Fluor 488-conjugated OVA, 25% of whole OVA) were prepared to quantify the uptake of OVA. As shown in Figure S5, the uptake of both liposomes was observed at 6 and 24 hr after treatment. Quantitative analysis revealed that the geometric mean values for the uptake of both liposomes were comparable after 5 hr, whereas the initial uptake speed (at 2 hr) was significantly higher in the case of the KALA-OVA-LPs (Figure S5A). The most significant difference was their homogeneity: the coefficient of variance (CV) for the cellular uptake of KALA-OVA-LPs was significantly lower compared with that of R8-OVA-LPs (Figure S5B). Furthermore, the difference in CV values became larger with increasing time, dominantly because of the increase in the corresponding value specifically in R8-OVA-LPs. This difference might be relevant with the anti-tumor effect of the immunization of ex vivo antigen-treated cells (Figure S4).

To elucidate the behavior of the liposomes in vivo, flow cytometric analyses of draining lymph nodes were performed after a subcutaneous (s.c.) injection of the liposomes. As a result, both liposomes, which were labeled with a fluorescently labeled lipid, were found to have accumulated in the draining lymph nodes at comparable levels (Figure S6A). Furthermore, although a large fraction of the liposomes were taken up by $CD11c^{-}F4/80^{-}$ cells, which were expected to be B cells, a portion of the liposomes were taken up by $CD11c^{+}F4/80^{+}$ cells, which are likely dendritic cells or macrophages (Figure S6B). Importantly, the level of in vivo cellular uptake to these cells was comparable between the KALA-OVA-LPs and the R8-OVA-LPs. These results suggest that the uptake process was not a major determinant for explaining the difference in the in vivo antigen-specific immune response between the KALA-OVA-LPs and R8-OVA-LPs.

To investigate the membrane-fusogenic activity of the KALA-OVA-LPs and the R8-OVA-LPs under conditions of physiological or endosomal pH, the membrane disruption activity of red blood cells (RBCs) was monitored after incubation with the liposomes by measuring the amount of hemoglobin that was released into the supernatant. In this experiment, RBCs were mixed with various amounts of liposomes in PBS adjusted to pH 5.5, 6.5, and 7.4, mimicking late endosomes,

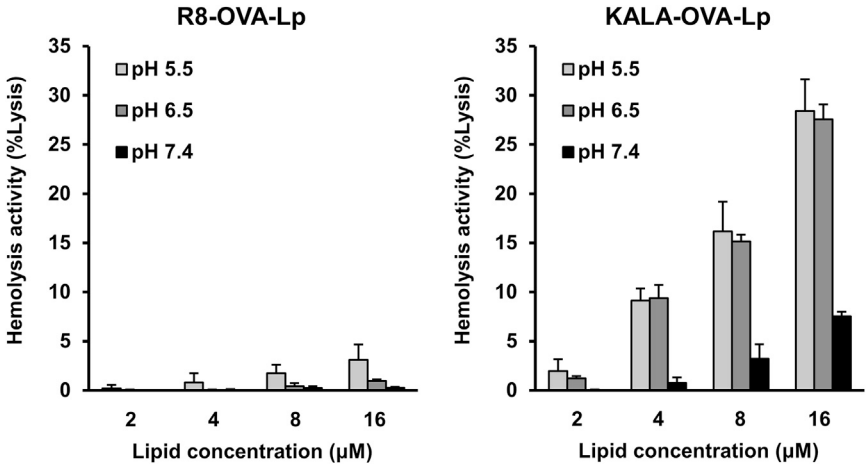

Figure 4. pH-Dependent Membrane Destabilization Activity of the KALA-OVA-LPs and the R8-OVA-LPs
RBCs were incubated with the KALA-OVA-LPs and the R8-OVA-LPs at various pH values for 30 min at 37°C. The values are represented as relative values of the positive control acquired by Triton X-100 treatment. Data are mean + SD (n = 3).

early/recycling endosomes, and the cytoplasm/extracellular space, respectively.[27] As a result, the KALA-OVA-LPs induced membrane disruption depending on the lipid concentration at pH 5.5 and 6.5, whereas membrane disruption was marginal in the case of the R8-OVA-LPs (Figure 4). Furthermore, antigen presentation in the presence of chloroquine, an endosome disruptive agent, was evaluated to investigate whether the membrane disruptive activity of the KALA peptide amplifies antigen presentation. Chloroquine treatment enhanced antigen presentation in cells that were treated with the R8-OVA-LPs, whereas the activity of the KALA-OVA-LPs was not enhanced but rather decreased (Figure 5). These results suggest that modifying liposomes with the KALA peptide induced a higher fusion with biomembranes in comparison with R8, especially under acidic pH conditions.

Immunological Analysis of the Mice Immunized with the KALA-OVA-LPs

To clarify the precise mechanism responsible for the immune response induced by the KALA-OVA-LPs, we performed further immunological analyses in vivo. We first evaluated the contribution of CD8- and CD4-positive T cells to the final output of in vivo CTL activity by depleting these cells using an antibody (Figure 6A). Mice were immunized with the KALA-OVA-LPs on day 0, and subsequently, 200 μg of an anti-CD4 or anti-CD8 antibody was injected intraperitoneally on days −1, 1, 3, and 6. OVA-specific CTL activity was evaluated 1 week after immunization by an in vivo CTL assay. Almost all of the CD4 or CD8 T cells were depleted on day 7. As a result, CD4 depletion failed to attenuate the CTL activity induced by the KALA-OVA-LPs but rather slightly enhanced the effect. In contrast, CD8 depletion drastically impaired CTL activity. These collective results suggest that CD4 T cells were not involved in the antigen-specific CTL activity induced by the KALA-OVA-LPs. Thereafter, we also evaluated the number of OVA-specific T cells induced by immunization with the KALA-OVA-LPs and R8-OVA-LPs by staining for intracellular cytokines. To assess the frequency of OVA-specific $CD8^+$ T cells, splenocytes from immunized mice were isolated and stimulated by treatment with the $OVA_{257–264}$ peptide (MHC-I peptide) in the presence of a protein transport inhibitor, followed by staining for intracellular IFN-γ. As a result, immunization with the KALA-OVA-LPs significantly increased the frequency of IFN-γ^+CD8^+ T cells (Figure 6B). This is consistent with the fact that the KALA-OVA-LPs induced significant in vivo CTL activity via $CD8^+$ T cells (Figures 1 and 6A). Furthermore, stimulation of the $OVA_{323–339}$ peptide (MHC-II peptide) revealed that OVA-specific Th2 immunity was induced by immunization with KALA-OVA-LPs, whereas Th1 and Th17 was not (Figure 6C). Collectively, these results suggest that the numbers of OVA-specific $CD8^+$ T cells and $CD4^+$ (Th2 phonotype) were expanded as the result of immunization with the KALA-OVA-LPs.

DISCUSSION

In the present study, we report on the development of a system that permits the efficient delivery of an antigen for cancer immunotherapy using an α-helical peptide, KALA. In general, positively charged nanoparticles are inherently taken up by a variety of cells, because they bind easily to the cell surface, which is negatively charged and covered by anionic proteoglycans.[28,29] Consistent with previous observations, both KALA-OVA-LPs and R8-OVA-LPs were efficiently taken up by BMDCs (Figure S5A). However, KALA-OVA-LPs were taken up more homogeneously in comparison with R8-OVA-LPs (Figure S5B). Because the surface charges and ζ potentials of both particles (prepared with DOPE as a helper lipid) were quite comparable, these differences cannot be simply explained by the physicochemical characteristics. One possible reason is the differences in secondary structure (i.e., an α-helical structure). As reported previously, the KALA peptide forms an α-helical structure when the liposomal membrane exists, whereas the oligo-arginine peptide (especially in R8 and R9) forms a random coil structure.[21,30,31] Several previous studies have reported that the α-helical structure interacts with glycosaminoglycans, whose binding is independent of electrostatic interactions.[32,33] Although these electrostatic and structural interactions might contribute to the efficient and homogeneous uptake of the KALA-OVA-LPs in BMDCs, the extent of accumulation in the lymph node between the KALA-OVA-LPs and the R8-OVA-LPs was comparable in vivo (Figure S6). Thus, the homogeneous uptake of the KALA-OVA-LPs might only contribute to applications of ex vivo protein vaccines (Figure S4).

The most drastic difference between the KALA-OVA-LPs and R8-OVA-LPs was their membrane-fusogenic activity, especially at acidic

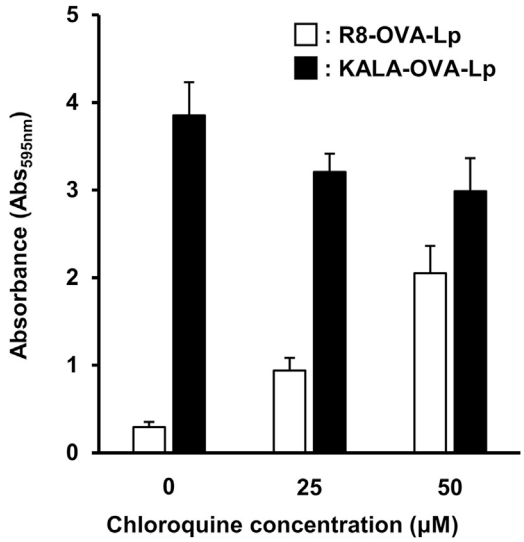

Figure 5. Antigen Presentation Activity in the Presence of Chloroquine, an Endosome-Disruptive Agent

BMDCs were pre-incubated with 0, 25, and 50 μM chloroquine in medium, followed by treatment of the KALA-OVA-LPs or the R8-OVA-LPs at a lipid dose of 32 μM. After 5 hr, the treated cells were co-cultured with a B3Z T cell hybridoma for 15 hr at 37°C. The co-cultured cells were lysed and incubated with chrolophenol red β-D-galactopyranoside buffer for 4 hr at 37°C. The absorbance at 595 nm was used as an index for antigen presentation activity. Data are mean + SD (n = 6).

conditions (Figure 4). It is plausible that this ability contributes to the remarkable induction of antigen presentation by KALA-OVA-LPs (Figure 3) because this process is prerequisite for MHC class I antigen presentation to release the antigen into the cytoplasm by overcoming endosome/lysosomes membranes. The experiments using chloroquine also strongly suggest that the KALA peptide amplifies endosomal escape, followed by the higher cytosolic delivery of antigen protein to a higher degree in comparison with R8 (Figure 5). However, the reason why the fusogenic ability of KALA was elicited at acidic conditions remains to be determined. Of note, the data reported herein are quite inconsistent with an original design and function of KALA peptide: it formed an α-helix at physiological pH. In fact, we also developed KALA-MEND to allow the encapsulating pDNA to enter the nucleus via stepwise membrane fusion with the plasma membrane and the nuclear membrane at cytoplasmic pH of 7.4. Thus, the prominently higher gene transfection of the KALA-MEND was not derived from the nuclear membrane fusion-mediated nuclear delivery of pDNA, as we designed.[19] Wyman et al.[21] reported that the KALA peptide can form an α-helical structure even under conditions of acidic pH, when the peptide is present with liposomes, whereas its structure changed to a random coil without liposomes. Therefore, it is highly possible that the KALA might form a α helix when it is modified onto the lipid envelope. Therefore, the pH-dependent membrane-fusogenic activity can be explained by assuming that the membrane-fusogenic activity might be perturbed via electrostatic interactions between KALA and the negatively charged helper lipid (CHEMS) that is incorporated in the liposomal component. However, when the KALA-LPs were exposed in an acidic pH in a range close to its pKa (~5.8), the fraction of ionized CHEMS is decreased by the protonation of the carboxyl group. In this situation, the electrostatic interactions become less intense, and the fusogenic function of KALA would be recovered. Such a pH-dependent loss of negative charge was conventionally used as a trigger for endosomal membrane fusion via the formation of an inverted hexagonal H_{II} phase in liposomes composed of DOPE, a cone-shape lipid, and CHEMS.[34,35] Collectively, the KALA-OVA-LPs might achieve an accelerated endosomal escape via a dual mechanism in response to pH via the protonation of CHEMS: switching on the KALA function by cancelling the electrostatic interactions with the peptide, and the loss of lamellar structure to form an inverse cone packaging formation for membrane fusion. Another possible reason is the presence of a histidine (His) residue in KALA. It is known that a His residue can be used to facilitate viral membrane fusion in response to low pH in some α-helical viral proteins.[36,37] Further investigations will be needed in order to clarify the effect of His residues on the membrane-fusogenic property of the KALA peptide.

As shown in Figures 1 and 3A, the induction of CTL activity and antigen presentation was weak in EPC-based liposomes, presumably because EPC-based liposome lacks membrane-fusogenic activity. Phosphatidylcholine derivatives, including EPC, are considered to be a stabilizer of lipid bilayers, because they form a cylindrical structure in the lipid membrane. Thus, it is difficult to overcome the endosomal membrane barrier, and subsequently for the antigen to be released to the cytoplasm. In support of this, we previously demonstrated that KALA-modified DOPE liposomes that encapsulate pDNA could stimulate the BMDCs via the stimulation of cytosolic DNA sensors, whereas the EPC-based liposome showed no activity.[20] Thus, EPC is inadequate in terms of cytoplasmic delivery, at least when used in combination with KALA peptides.

As shown in Figure 3, KALA-OVA-LPs induced potent antigen presentation in BMDCs. In addition, subsequent immunization with these DCs (ex vivo immunization) efficiently inhibited tumor growth in comparison with those of R8-OVA-LP-treated BMDCs (Figure S4). However, this ex vivo approach conferred less anti-tumor effect in comparison with a direct in vivo immunization of KALA-OVA-LPs: the complete prevention of the tumor growth was observed up to day 15 after tumor inoculation (Figure 2A). These data suggest that DCs are not a unique cell population that contributes to the anti-tumor effect of the KALA-OVA-LPs in vivo. One of the considerable populations is macrophages, a type of APC as well as DCs. In fact, while the large fraction of the liposomes was taken up by $CD11c^{-}F4/80^{-}$ cells, which have the characteristics of B cells, a part of the liposomes was taken up by $CD11c^{+}F4/80^{+}$ cells, which is considered to be dendritic cells/macrophages (Figure S6B). It is generally thought that the DCs are major, even unique, APCs that can activate naive T cells, and macrophages are considered to be less potent APCs in terms of their activation. However, an accumulating body of evidence has revealed that a specific subpopulation of macrophages in lymph nodes, CD169-positive macrophages,

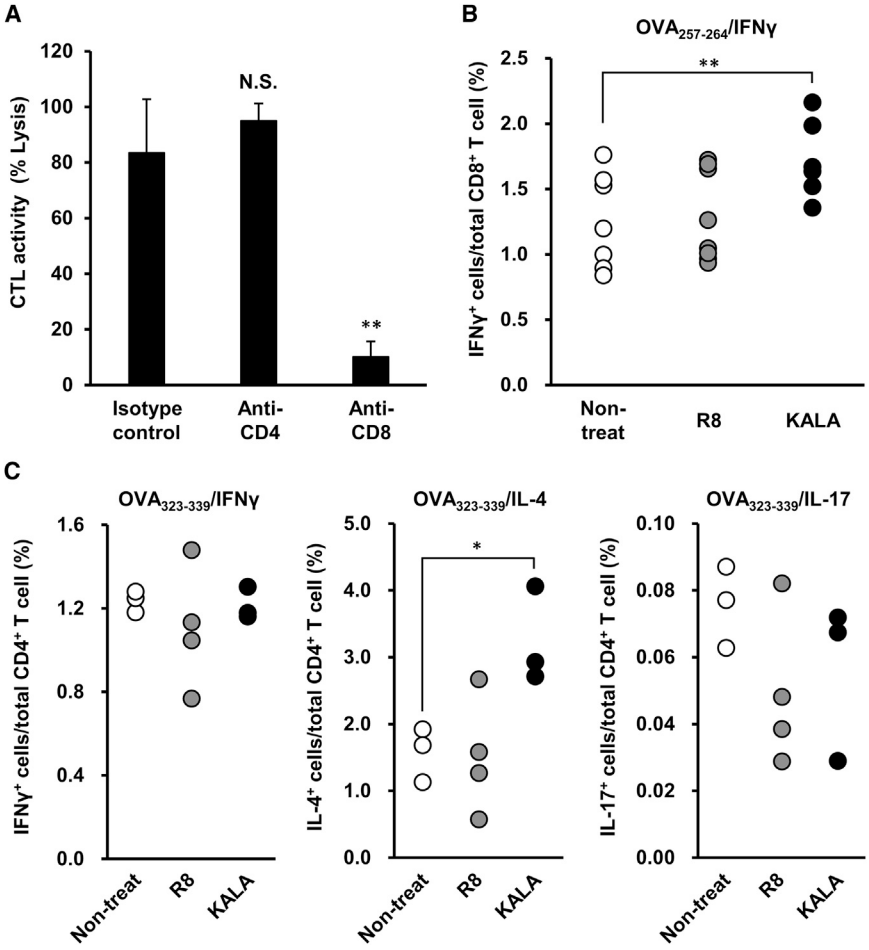

Figure 6. Immunological Analysis of the Mice Immunized with the KALA-OVA-LPs

(A) C57BL/6J mice were immunized subcutaneously once with KALA-OVA-LPs at a dose of 25 μg OVA. At 1 days before and 1, 3, and 6 days after the immunization, anti-CD4, anti-CD8, or isotype control antibody was intraperitoneally administered at a dose of 200 μg. Fluorescent-labeled target cells ($OVA_{257–264}$ pulsed, $CFSE^{High}$) and control cells (no peptide pulsed, $CFSE^{Low}$) were injected intravenously at 1 week after immunization. The OVA-specific lysis was calculated from the target cell/control cell ratio measured by flow cytometer 20 hr after injection. Data are mean + SEM (n = 3). Statistical analysis was performed using one-way ANOVA, followed by the Bonferroni test. **p < 0.01 versus isotype control group. (B and C) C57BL/6J mice were immunized subcutaneously with KALA-OVA-LPs at a dose of 25 μg OVA twice every 7 days. At 7 days after the second immunization, splenocytes were harvested and re-stimulated by (B) $OVA_{257–264}$ or (C) $OVA_{323–339}$, followed by an additional incubation with the protein transport inhibitor. Populations of cells in the spleen, which were positive in IFNγ (B and C), IL-4, and IL-17 (C) were quantified by flow cytometry after the immunostaining for intracellular cytokines. Each dot represents the percentage of cytokine-positive cells in an individual mouse. Statistical analysis was performed using one-way ANOVA, followed by the Bonferroni test. *p < 0.05 and **p < 0.01 versus non-treated group.

contribute to the antigen-specific CTL response and subsequent anti-tumor effect.[38–40] For example, Muraoka et al.[40] revealed that an antigen peptide encapsulated within a nanoparticulate hydrogel (nanogel, composed of cholesteryl pullulan) was efficiently incorporated into CD169-positive medullary macrophages and elicited a potent anti-tumor effect. Although a cationic nanogel was reported to be less incorporated into macrophages in draining lymph nodes in comparison with neutral ones, it has also been reported that a cationic agarose hydrogel could deliver incorporated nucleic acids into CD169-positive macrophages.[41] These facts suggest that macrophages, in particular CD169-positive macrophages, may contribute to the anti-tumor effect of KALA-OVA-LPs in vivo. Additional strategies for targeting draining lymph nodes may improve the efficiency of the KALA-OVA-LPs, such as PEGylation for shielding the surface charge to avoid trapping by the extracellular matrix or ligand modification for the targeting of the specific cell type.[42,43]

In conclusion, we report herein on the development of a carrier for delivering an antigen protein that has the potential for use in cancer immunotherapy. Modifying antigen-encapsulating liposomes with KALA facilitated antigen-specific CTL activity and anti-tumor effects when the liposomes were administered subcutaneously. Furthermore, OVA-specific $CD8^+$ T cells and $CD4^+$ cells (Th2 phenotype) were expanded by immunization with the KALA-OVA-LPs. Considering that $CD4^+$ T cells were not involved in OVA-specific CTL activity induced by the KALA-OVA-LPs (Figure 6A), the activation of Th2 immunity might not be relevant with the activity of the KALA-OVA-LPs as an anti-cancer vaccine. However, this result suggests a possibility for application of KALA-OVA-LPs to infectious diseases via induction of humoral immunity. Experiments using BMDCs suggested that the KALA-OVA-LPs induced a much more potent OVA-specific MHC class I restricted antigen presentation in comparison with R8-OVA-LPs, which were reported to be a highly efficient carrier. This effect can be attributed to the cytoplasmic delivery of the antigen via the acidic environment-specific membrane destabilization activity in the KALA-OVA-LPs. Collectively, the KALA-modified antigen-encapsulating liposomes are promising devices for use as an anti-cancer vaccine, which can be combined with immune checkpoint inhibitors such as an anti-PD-1 antibody.

MATERIALS AND METHODS

Materials

DOPE and EPC were purchased from Avanti Polar Lipid. Cholesterol (Chol), CHEMS, and ovalbumin (grade VI) were purchased from Sigma. Alexa Fluor 488-conjugated OVA and 1,1′-dioctadecyl-3,3,3′,3′-tetramethylindodicarbocyanine,4-chlorobenzenesulfonate salt (DiD) were purchased from Invitrogen.

Chlorophenol red β-D-galactopyranoside was purchased from Roche Diagnostics. Stearylated octa-arginine (STR-R8) and stearylated KALA (STR-KALA) were custom-synthesized by Kurabo as described previously.[21] Mouse recombinant granulocyte-macrophage stimulating factor (GM-CSF) and mouse IL-6 Quantikine ELISA were purchased from R&D Systems. Fluorescent dye-conjugated monoclonal antibodies, including F4/80 (clone: BM8; catalog no. 123109), CD11c (clone: N418; catalog no. 117305), CD3 (clone: 145-2C11; catalog no. 100311), CD4 (clone: RM4-5; catalog no. 100511), CD8 (clone: 53-6.7; catalog no. 100705), IFNγ (clone: XMG1.2; catalog no. 505807), IL-4 (clone: 11B11; catalog no. 504103), IL-17 (clone: TC11-18H10.1; catalog no.: 506903), CD80 (clone: 16-10A1; catalog no. 104707), CD86 (clone: GL-1; catalog no. 105007), isotype control antibody, and anti-mouse CD16/32 antibody (clone: 93; catalog no. 101302) were purchased from Biolegend. OVA H-2K^b cytotoxic T lymphocyte epitope peptide (SIINFEKL, $OVA_{257–264}$) was synthesized by TORAY Research Center. OVA H-2K^b helper T lymphocyte epitope peptide (ISQAVHAAHAEINEAGR, $OVA_{323–339}$) was synthesized by Invitrogen. All other chemicals were commercially available and reagent grade products.

Cell Lines

E.G7-OVA cells, a murine lymphoma cell line EL4 expressing chicken OVA, were purchased from the American Type Culture Collection. B3Z, a CD8$^+$ T cell hybridoma specific for the $OVA_{257–264}$ epitope in the context of K^{b,41},[26] was a generous gift from Dr. Shastri (University of California, Berkeley). These cells were cultured in RPMI-1640 medium containing 50 μM 2-mercaptethanol, 10 mM HEPES, 1 mM sodium pyruvate, 100 U/mL penicillin, 100 μg/mL streptomycin, and 10% fetal calf serum.

Preparation of KALA-OVA-LPs and R8-OVA-LPs

DOPE-based OVA-LPs were composed of DOPE, CHEMS, and EPC (75:1.25:23.75 molar ratio), and EPC based OVA-LPs were composed of EPC, CHEMS, and Chol (7:1:2). Each of the OVA-LPs was prepared by the lipid film hydration method, as reported previously, with minor modifications.[18] Briefly, a chloroform solution of lipids was mixed in a test tube, and the solvent was evaporated by a stream on nitrogen gas to produce a thin lipid film. The resulting lipid film was hydrated with a 5 mg/mL solution of OVA in 10 mM HEPES (pH 7.4) for 10 min at room temperature (300 μL, 10 mM of total lipid concentration). For fluorescence-activated cell sorting (FACS) analysis, 25% of the OVA was substituted by an Alexa Fluor 488-conjugated one. The hydrated lipid film was then gently sonicated to produce the liposomes. The liposome suspension was subjected to five freeze and thaw cycles. After the treatment, the liposome suspension was extruded through polycarbonate membrane filters (400-nm pore size; Nucleopore) with a Mini-extruder (Avanti Polar Lipids) for sizing the liposomes. To remove unencapsulated OVA, the liposome suspension was centrifuged at 80,000 × *g* for 30 min at 4°C. After purification of the liposomes, the surface of the liposomal membrane was modified with STR-KALA and STR-R8 (5 mol% of total lipids) by vortexing the liposome suspension. The diameter and ζ potential of the liposomes were determined using an electrophoretic light-scattering spectrophotometer (Zetasizer; Malvern Instruments). The concentrations of lipid and protein were determined using a phospholipid assay kit (Wako) and a BCA protein assay kit (Pierce) after precipitation.[44]

Tumor Challenge

Female C57BL/6J (H-2^b) mice (6–8 weeks old) were obtained from Japan SLC. The protocol for using the mice was approved by the Pharmaceutical Science Animal Committee of Hokkaido University. In the prophylactic experiment, the mice were immunized with KALA-OVA-LPs, R8-OVA-LPs, unmodified OVA-LPs containing 25 μg OVA, and KALA-LPs (the same amount of lipid as KALA-OVA-LPs) subcutaneously. At 7 days after immunization, the left flanks of the mice were subcutaneously inoculated with 8.0×10^5 E.G7-OVA cells. In the therapeutic experiment, the mice were subcutaneously inoculated in the left flank with 8.0×10^5 E.G7-OVA cells. At 5, 9, 13, and 17 days after tumor inoculation, the mice were subcutaneously immunized with the KALA-OVA-LPs containing 25 μg OVA. Anti-PD-1 or isotype control antibody (clone: RMP1-14, 2A3; catalog nos. BE0146, BE0089, respectively; BioXCell) also administered intraperitoneally at a dose of 50 μg at 2 day intervals after the immunization. Tumor volume was calculated using the following formula: major axis × (minor axis)^2 × 0.52.

In Vivo CTL Assay

In vivo CTL assays were performed as described previously.[45] Briefly, C57BL/6J mice were subcutaneously immunized with each sample. In the CD4/CD8 depletion experiments, 200 μg of anti-CD4, CD8, or isotype control antibody (clone: YTS 191, YTS 169.4, and LTF-2; catalog nos. BE0119, BE0117, and BE0090, respectively; BioXcell) was administered intraperitoneally at 1 day before and 1, 3, and 6 days after immunization. After 7 days, splenocytes were prepared from naive C57BL/6J mice and incubated for 1 hr at 37°C with the $OVA_{257–264}$ peptide in RPMI-1640 medium containing 50 μM 2-mercaptethanol, 10 mM HEPES, 1 mM sodium pyruvate, 100 U/mL penicillin, 100 μg/mL streptomycin, and 10% fetal calf serum. The $OVA_{257–264}$ peptide-presented splenocytes were then labeled by incubation for 10 min at 37°C with 5 μM carboxyfluorescein succinimidyl ester (CFSE) in PBS (CFSE^{High} cells). The naive splenocytes were labeled by incubation for 10 min at 37°C with 0.5 μM CFSE in PBS (CFSE^{Low} cells). CFSE-labeled cells were washed with PBS. A mixture of 5×10^6 cells CFSE^{High} cells and 5×10^6 cells CFSE^{Low} cells was intravenously injected into the immunized mice. After 20 hr, splenocytes from immunized mice were collected, and single-cell suspensions were analyzed for the detection and quantification of CFSE-labeled cells by FACSCaliber (BD). The numbers of CFSE^{Low} cells were essentially the same in all samples, including the non-treated group. The values for lysis were the number of CFSE^{High} cells corrected by the number of CFSE^{Low} cells. In this study, no non-specific lysis was observed.

Measurement of IL-6 Concentration in Serum

The KALA-OVA-LPs and the R8-OVA-LPs were subcutaneously injected to the backs of C57BL/6J mice. After 1, 3, 6, 12, and 24 hr,

blood was collected from the tail vein, followed by centrifugation at 2,000 × *g*, for 10 min at 4°C to obtain serum samples. IL-6 concentration of the serum was measured using a Mouse IL-6 Quantikine ELISA Kit.

Lymph Nodes Accumulation of the Liposomes

To evaluate the lymph node accumulation of each of the OVA-LPs, 0.1 mol% DiD-labeled each OVA-LPs were subcutaneously injected to the left and right flanks of C57BL6/J mice. After 24 hr, inguinal lymph nodes were collected, mashed, and filtered through a nylon mesh. The acquired cell suspension was washed with FACS buffer twice, followed by Fc-blocking (anti-CD16/32 antibody) and staining with PE-conjugated anti-F4/80 (2.5 μg/mL) and fluorescein isothiocyanate (FITC)-conjugated CD11c (5.0 μg/mL) antibody. After washing, the cells were analyzed by FACSAriaII (Becton Dickinson). Dead cells were removed by means of a 7-AAD Viability Staining Solution (Biolegend).

Preparation of Mouse BMDCs

BMDCs of mice were prepared as described previously.[18] Briefly, bone marrow cells were cultured overnight in RPMI-1640 medium containing 50 μM 2-mercaptethanol, 10 mM HEEPS, 1 mM sodium pyruvate, 100 U/mL penicillin, 100 μg/mL streptomycin, and 10% fetal calf serum. Non-adherent cells were harvested and cultured in the same medium supplemented with 10 ng/mL GM-CSF. On days 2 and 4, non-adherent cells were removed, and the remaining adherent cells were cultured in fresh medium containing 10 ng/mL GM-CSF. On day 6, non-adherent cells were used in the experiment as immature BMDCs.

Antigen Presentation Assay

BMDCs (1.0×10^6 cells) were incubated with each OVA-LP at an indicated lipid concentration for 2 hr at 37°C in serum-free RPMI-1640 medium. RPMI-1640 medium was then added to the cells, followed by a further 3 hr of incubation. GM-CSF was added in the medium at 10 ng/mL throughout the incubation. In the chloroquine experiments, the BMDCs were incubated with medium containing chloroquine for 30 min before being incubated with the liposomes. The treated BMDCs were harvested by pipetting, followed by centrifugation at 500 × *g*, for 5 min. The BMDCs (2.0×10^5 cells) were mixed with B3Z (1.0×10^5 cells) and co-cultured in RPMI-1640 with 10% fetal calf serum (FCS) in a 96-well plate at 37°C for 15 hr. The co-cultured cells were washed with PBS, followed by incubation with 100 μL chlorophenol red β-D-garactopyranoside buffer (5 mM chlorophenol red β-D-garactopyranoside, 0.125% NP-40, and 9 mM $MgCl_2$ in PBS) for 4 hr at 37°C. After the incubation, the absorbance at 595 nm of each well was measured using a microplate reader (Benchmark Plus; BioRad).

Flow Cytometric Analysis of BMDCs

To evaluate the kinetics of uptake of each OVA-LP, BMDCs were incubated with the OVA-LPs encapsulated Alexa Fluor 488-conjugated OVA in serum-free RPMI-1640 for 2 hr, followed by a further 0, 4, 10, and 22 hr (total incubation time was 2, 6, 12, and 24 hr, respectively). GM-CSF was added in the medium at 10 ng/mL throughout the incubation. After the incubation, the cells were harvested by pipetting, followed by washing with RPMI-1640 medium two times and PBS containing 0.5% BSA and 0.1% NaN_3 (FACS buffer) two times. After washing, the BMDCs were analyzed using FACSCaliber.

Hemolysis Assay

Hemolysis assays were performed as described previously, with minor modifications.[46] Briefly, male ICR mice (4–6 weeks old) were obtained from Japan SLC. Fresh red blood cells were collected from ICR mice and suspended in PBS (pH 7.4) or 10 mM malic acid/PBS (pH 5.5 or 6.5). The RBC suspension was mixed with indicated concentration of OVA-LPs and then incubated at 37°C for 30 min. After the incubation, the absorbance of the supernatant at 545 nm was measured after centrifugation at 500 × *g*, for 5 min. The RBCs lysed by incubation with 0.02% w/v Triton-X was used as a positive control. As a negative control, the RBCs without OVA-LPs were also measured. The percentage lysis was represented as the percentage of the absorbance of positive control.

Intracellular Cytokine Staining Assay

C57BL/6J mice were immunized with the KALA-OVA-LPs or the R8-OVA-LPs at a dose of 25 μg OVA twice every 7 days. At 7 days after the second immunization, splenocytes were harvested and incubated with 1 mM $OVA_{257–264}$ (for MHC class I stimulation) or $OVA_{323–339}$ (for MHC class II stimulation) for 1 hr at 37°C, followed by an additional 6 hr of incubation with GoldiPlug (BD). Cells were treated with anti-mouse CD16/32 antibody to block non-specific antibody binding, followed by staining the surface markers with APC-conjugated anti-CD3 (2.5 μg/mL) and FITC-conjugated anti-CD4 or CD8 (2.5 μg/mL) antibody in FACS buffer for 30 min at 4°C. Permeabilization and fixation was then performed using the Transcription Factor Buffer Set (BD) according to the manufacturer's protocol. Briefly, the stained cells were incubated in the Fix/Perm Working Solution for 45 min at 4°C. The cells were then washed twice with the Perm/Wash Working Solution, followed by staining the intracellular cytokines by PE-conjugated anti-IFNγ, IL-4, or IL-17 (1.2 μg/mL) antibody in Perm/Wash Working Solution for 45 min at 4° and analyzed using FACSAriaII (BD).

Statistical Analysis

Comparisons between multiple treatments were performed by one-way ANOVA, followed by Bonferroni correction. Comparisons between two treatments were performed using unpaired Student's t test. A p value < 0.05 was considered to indicate a significant difference.

SUPPLEMENTAL INFORMATION

Supplemental Information includes six figures and can be found with this article online at http://dx.doi.org/10.1016/j.ymthe.2017.01.020.

AUTHOR CONTRIBUTIONS

N.M. and N.T. performed the experiments. N.M. and H.A. analyzed data and wrote the manuscript with critical input from the coauthors. H.A., T.N., and H.H. supervised the project and designed experiments. All authors contributed to discussing the results. All authors have given approval to the final version of the manuscript.

CONFLICTS OF INTEREST

The authors declare no conflict of interest.

ACKNOWLEDGMENTS

This work was supported by JSPS KAKENHI grants 15H01806 and 15K14934, The Mochida Memorial Foundation for Medical and Pharmaceutical Research, The Asahi Glass Foundation, and Takeda Science Foundation. We wish to thank Dr. M.S. Feather for his helpful advice in writing the English manuscript.

REFERENCES

1. Tacken, P.J., de Vries, I.J., Torensma, R., and Figdor, C.G. (2007). Dendritic-cell immunotherapy: from ex vivo loading to in vivo targeting. Nat. Rev. Immunol. *7*, 790–802.
2. Apostolopoulos, V., Pietersz, G.A., Gordon, S., Martinez-Pomares, L., and McKenzie, I.F. (2000). Aldehyde-mannan antigen complexes target the MHC class I antigen-presentation pathway. Eur. J. Immunol. *30*, 1714–1723.
3. Zhou, F., and Huang, L. (1995). Delivery of protein antigen to the major histocompatibility complex class I-restricted antigen presentation pathway. J. Drug Target. *3*, 91–109.
4. Laus, R., Graddis, T.J., Hakim, I., and Vidovic, D. (2000). Enhanced major histocompatibility complex class I-dependent presentation of antigens modified with cationic and fusogenic peptides. Nat. Biotechnol. *18*, 1269–1272.
5. Joffre, O.P., Segura, E., Savina, A., and Amigorena, S. (2012). Cross-presentation by dendritic cells. Nat. Rev. Immunol. *12*, 557–569.
6. Joshi, M.D., Unger, W.J., Storm, G., van Kooyk, Y., and Mastrobattista, E. (2012). Targeting tumor antigens to dendritic cells using particulate carriers. J. Control. Rel. *161*, 25–37.
7. Tahara, Y., and Akiyoshi, K. (2015). Current advances in self-assembled nanogel delivery systems for immunotherapy. Adv. Drug Deliv. Rev. *95*, 65–76.
8. Almeida, A.J., and Souto, E. (2007). Solid lipid nanoparticles as a drug delivery system for peptides and proteins. Adv. Drug Deliv. Rev. *59*, 478–490.
9. Schwendener, R.A. (2014). Liposomes as vaccine delivery systems: a review of the recent advances. Ther. Adv. Vaccines *2*, 159–182.
10. Altin, J.G., and Parish, C.R. (2006). Liposomal vaccines—targeting the delivery of antigen. Methods *40*, 39–52.
11. Moon, J.J., Suh, H., Bershteyn, A., Stephan, M.T., Liu, H., Huang, B., Sohail, M., Luo, S., Um, S.H., Khant, H., et al. (2011). Interbilayer-crosslinked multilamellar vesicles as synthetic vaccines for potent humoral and cellular immune responses. Nat. Mater. *10*, 243–251.
12. van Broekhoven, C.L., Parish, C.R., Demangel, C., Britton, W.J., and Altin, J.G. (2004). Targeting dendritic cells with antigen-containing liposomes: a highly effective procedure for induction of antitumor immunity and for tumor immunotherapy. Cancer Res. *64*, 4357–4365.
13. Faham, A., and Altin, J.G. (2010). Antigen-containing liposomes engrafted with flagellin-related peptides are effective vaccines that can induce potent antitumor immunity and immunotherapeutic effect. J. Immunol. *185*, 1744–1754.
14. Arigita, C., Bevaart, L., Everse, L.A., Koning, G.A., Hennink, W.E., Crommelin, D.J., van de Winkel, J.G., van Vugt, M.J., Kersten, G.F., and Jiskoot, W. (2003). Liposomal meningococcal B vaccination: role of dendritic cell targeting in the development of a protective immune response. Infect. Immun. *71*, 5210–5218.
15. Kawasaki, N., Rillahan, C.D., Cheng, T.Y., Van Rhijn, I., Macauley, M.S., Moody, D.B., and Paulson, J.C. (2014). Targeted delivery of mycobacterial antigens to human dendritic cells via Siglec-7 induces robust T cell activation. J. Immunol. *193*, 1560–1566.
16. Xiao, K., Li, Y., Luo, J., Lee, J.S., Xiao, W., Gonik, A.M., Agarwal, R.G., and Lam, K.S. (2011). The effect of surface charge on in vivo biodistribution of PEG-oligocholic acid based micellar nanoparticles. Biomaterials *32*, 3435–3446.
17. Oh, W.K., Kim, S., Choi, M., Kim, C., Jeong, Y.S., Cho, B.R., Hahn, J.S., and Jang, J. (2010). Cellular uptake, cytotoxicity, and innate immune response of silica-titania hollow nanoparticles based on size and surface functionality. ACS Nano *4*, 5301–5313.
18. Nakamura, T., Moriguchi, R., Kogure, K., Shastri, N., and Harashima, H. (2008). Efficient MHC class I presentation by controlled intracellular trafficking of antigens in octaarginine-modified liposomes. Mol. Ther. *16*, 1507–1514.
19. Akita, H., Ishii, S., Miura, N., Shaheen, S.M., Hayashi, Y., Nakamura, T., Kaji, N., Baba, Y., and Harashima, H. (2013). A DNA microarray-based analysis of immune-stimulatory and transcriptional responses of dendritic cells to KALA-modified nanoparticles. Biomaterials *34*, 8979–8990.
20. Miura, N., Shaheen, S.M., Akita, H., Nakamura, T., and Harashima, H. (2015). A KALA-modified lipid nanoparticle containing CpG-free plasmid DNA as a potential DNA vaccine carrier for antigen presentation and as an immune-stimulative adjuvant. Nucleic Acids Res. *43*, 1317–1331.
21. Wyman, T.B., Nicol, F., Zelphati, O., Scaria, P.V., Plank, C., and Szoka, F.C., Jr. (1997). Design, synthesis, and characterization of a cationic peptide that binds to nucleic acids and permeabilizes bilayers. Biochemistry *36*, 3008–3017.
22. Ahmed, K.K., Geary, S.M., and Salem, A.K. (2016). Development and evaluation of biodegradable particles coloaded with antigen and the Toll-like receptor agonist, pentaerythritol lipid A, as a cancer vaccine. J. Pharm. Sci. *105*, 1173–1179.
23. Kurosaki, T., Kitahara, T., Nakamura, T., Nishida, K., Fumoto, S., Kodama, Y., Nakagawa, H., Higuchi, N., and Sasaki, H. (2012). Development of effective cancer vaccine using targeting system of antigen protein to APCs. Pharm. Res. *29*, 483–489.
24. Guermonprez, P., Valladeau, J., Zitvogel, L., Théry, C., and Amigorena, S. (2002). Antigen presentation and T cell stimulation by dendritic cells. Annu. Rev. Immunol. *20*, 621–667.
25. Banchereau, J., and Steinman, R.M. (1998). Dendritic cells and the control of immunity. Nature *392*, 245–252.
26. Shastri, N., and Gonzalez, F. (1993). Endogenous generation and presentation of the ovalbumin peptide/Kb complex to T cells. J. Immunol. *150*, 2724–2736.
27. Casey, J.R., Grinstein, S., and Orlowski, J. (2010). Sensors and regulators of intracellular pH. Nat. Rev. Mol. Cell Biol. *11*, 50–61.
28. Mislick, K.A., and Baldeschwieler, J.D. (1996). Evidence for the role of proteoglycans in cation-mediated gene transfer. Proc. Natl. Acad. Sci. U S A *93*, 12349–12354.
29. Shin, E.H., Li, Y., Kumar, U., Sureka, H.V., Zhang, X., and Payne, C.K. (2013). Membrane potential mediates the cellular binding of nanoparticles. Nanoscale *5*, 5879–5886.
30. Takechi, Y., Yoshii, H., Tanaka, M., Kawakami, T., Aimoto, S., and Saito, H. (2011). Physicochemical mechanism for the enhanced ability of lipid membrane penetration of polyarginine. Langmuir *27*, 7099–7107.
31. Eiríksdóttir, E., Konate, K., Langel, U., Divita, G., and Deshayes, S. (2010). Secondary structure of cell-penetrating peptides controls membrane interaction and insertion. Biochim. Biophys. Acta *1798*, 1119–1128.
32. Tchoumi Neree, A., Nguyen, P.T., Chatenet, D., Fournier, A., and Bourgault, S. (2014). Secondary conformational conversion is involved in glycosaminoglycans-mediated cellular uptake of the cationic cell-penetrating peptide PACAP. FEBS Lett. *588*, 4590–4596.
33. Yang, J., Tsutsumi, H., Furuta, T., Sakurai, M., and Mihara, H. (2014). Interaction of amphiphilic α-helical cell-penetrating peptides with heparan sulfate. Org. Biomol. Chem. *12*, 4673–4681.
34. Ellens, H., Bentz, J., and Szoka, F.C. (1984). pH-induced destabilization of phosphatidylethanolamine-containing liposomes: role of bilayer contact. Biochemistry *23*, 1532–1538.

35. Lee, R.J., and Huang, L. (1996). Folate-targeted, anionic liposome-entrapped polylysine-condensed DNA for tumor cell-specific gene transfer. J. Biol. Chem. *271*, 8481–8487.

36. Kampmann, T., Mueller, D.S., Mark, A.E., Young, P.R., and Kobe, B. (2006). The role of histidine residues in low-pH-mediated viral membrane fusion. Structure *14*, 1481–1487.

37. Krishnan, A., Verma, S.K., Mani, P., Gupta, R., Kundu, S., and Sarkar, D.P. (2009). A histidine switch in hemagglutinin-neuraminidase triggers paramyxovirus-cell membrane fusion. J. Virol. *83*, 1727–1741.

38. Martinez-Pomares, L., and Gordon, S. (2012). CD169+ macrophages at the crossroads of antigen presentation. Trends Immunol. *33*, 66–70.

39. Asano, K., Nabeyama, A., Miyake, Y., Qiu, C.H., Kurita, A., Tomura, M., Kanagawa, O., Fujii, S., and Tanaka, M. (2011). CD169-positive macrophages dominate antitumor immunity by crosspresenting dead cell-associated antigens. Immunity *34*, 85–95.

40. Muraoka, D., Harada, N., Hayashi, T., Tahara, Y., Momose, F., Sawada, S., Mukai, S.A., Akiyoshi, K., and Shiku, H. (2014). Nanogel-based immunologically stealth vaccine targets macrophages in the medulla of lymph node and induces potent antitumor immunity. ACS Nano *8*, 9209–9218.

41. Huang, Z., Zhang, Z., Zha, Y., Liu, J., Jiang, Y., Yang, Y., Shao, J., Sun, X., Cai, X., Yin, Y., et al. (2012). The effect of targeted delivery of anti-TNF-α oligonucleotide into CD169+ macrophages on disease progression in lupus-prone MRL/lpr mice. Biomaterials *33*, 7605–7612.

42. Zhuang, Y., Ma, Y., Wang, C., Hai, L., Yan, C., Zhang, Y., Liu, F., and Cai, L. (2012). PEGylated cationic liposomes robustly augment vaccine-induced immune responses: role of lymphatic trafficking and biodistribution. J. Control. Release *159*, 135–142.

43. Wang, C., Liu, P., Zhuang, Y., Li, P., Jiang, B., Pan, H., Liu, L., Cai, L., and Ma, Y. (2014). Lymphatic-targeted cationic liposomes: a robust vaccine adjuvant for promoting long-term immunological memory. Vaccine *32*, 5475–5483.

44. Brown, R.E., Jarvis, K.L., and Hyland, K.J. (1989). Protein measurement using bicinchoninic acid: elimination of interfering substances. Anal. Biochem. *180*, 136–139.

45. Yang, Y., Huang, C.T., Huang, X., and Pardoll, D.M. (2004). Persistent Toll-like receptor signals are required for reversal of regulatory T cell-mediated CD8 tolerance. Nat. Immunol. *5*, 508–515.

46. Sato, Y., Hatakeyama, H., Sakurai, Y., Hyodo, M., Akita, H., and Harashima, H. (2012). A pH-sensitive cationic lipid facilitates the delivery of liposomal siRNA and gene silencing activity in vitro and in vivo. J. Control. Release *163*, 267–276.

YMTHE, Volume *25*

Supplemental Information

Modifying Antigen-Encapsulating Liposomes with KALA Facilitates MHC Class I Antigen Presentation and Enhances Anti-tumor Effects

Naoya Miura, Hidetaka Akita, Naho Tateshita, Takashi Nakamura, and Hideyoshi Harashima

Supplementary Figure 1.

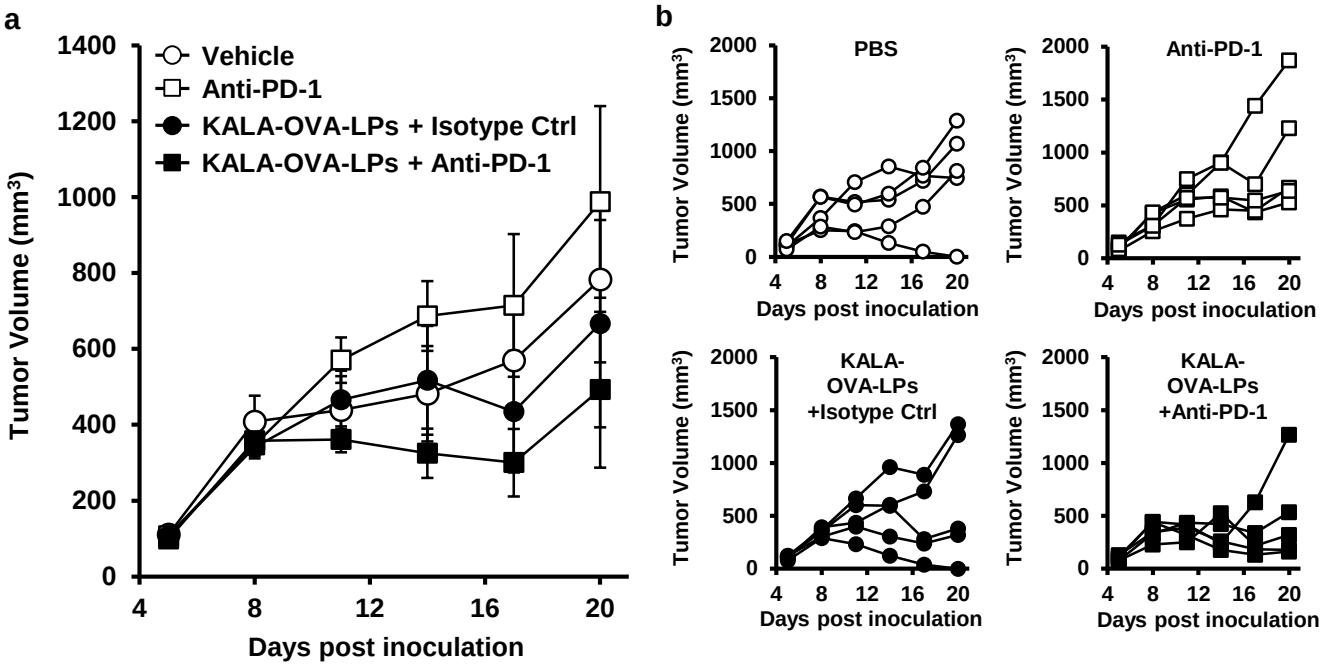

Supplementary Figure 1. Therapeutic anti-tumor effect combined with anti-PD-1 treatment
(a) C57BL/6 mice were inoculated with 8.0×10^5 cells of E.G7-OVA in the left flank. 5, 9, 13, 17 days after inoculation, mice were immunized subcutaneously with KALA-OVA-LPs at a dose of 25 μg OVA. Anti-PD-1 or Isotype Ctrl antibody was also administered intraperitoneally at a dose of 50 μg on every two days from first immunization. The tumor volume was measured up to 20 days after inoculation. The plots represent the mean ± SEM (n = 5). (b) Tumor volume of individual mouse of each group in the experiment (a).

Supplementary Figure 2.

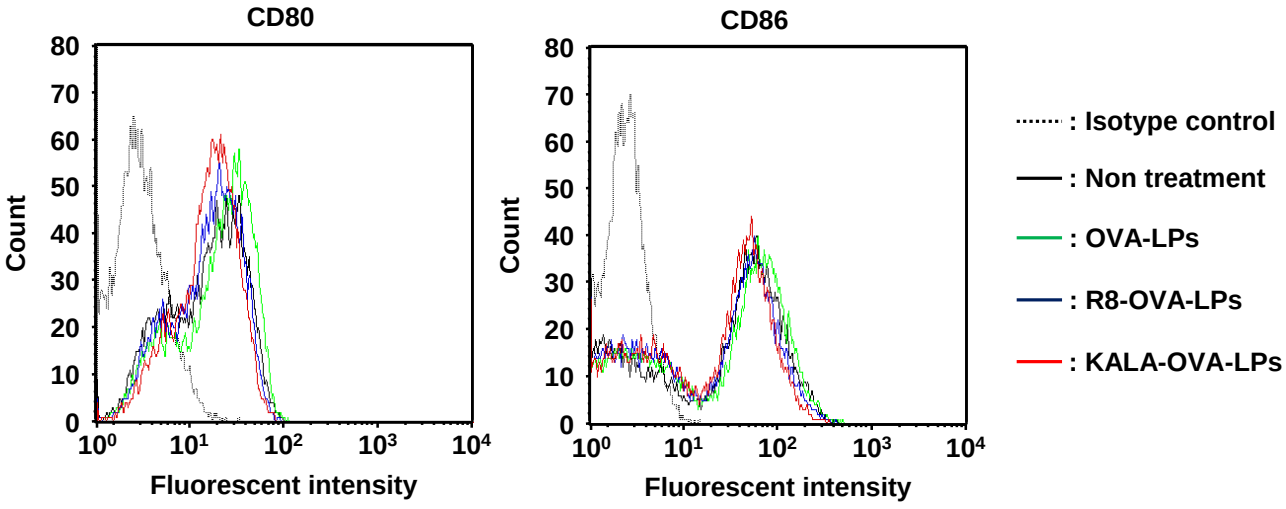

Supplementary Figure 2. CD80/86 expression in BMDCs that were treated with liposomes.
BMDCs (1.0×10^6 cells) were treated with the KALA-OVA-LPs, the R8-OVA-LPs or the non-modified OVA-LPs at a lipid dose of 32 μM. After 18 hours, the BMDCs were recovered and stained by PE-labeled anti-mouse CD80 and CD86 (Biolegend).

Supplementary Figure 3.

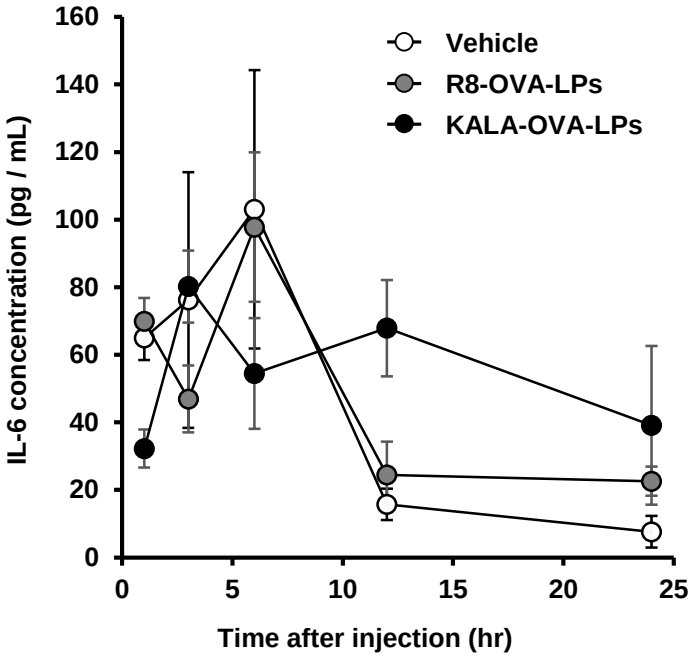

Supplementary Figure 3. IL-6 concentration in serum after liposome injection.
C57BL/6 mice were administered subcutaneously with KALA-OVA-LPs, R8-OVA-LPs at a dose of 25 μg OVA. Blood of these mice was collected at 1, 3, 6, 12 and 24 hrs after administration. Serum was separated from blood and the IL-6 concentration was measured by ELISA.

Supplementary Figure 4.

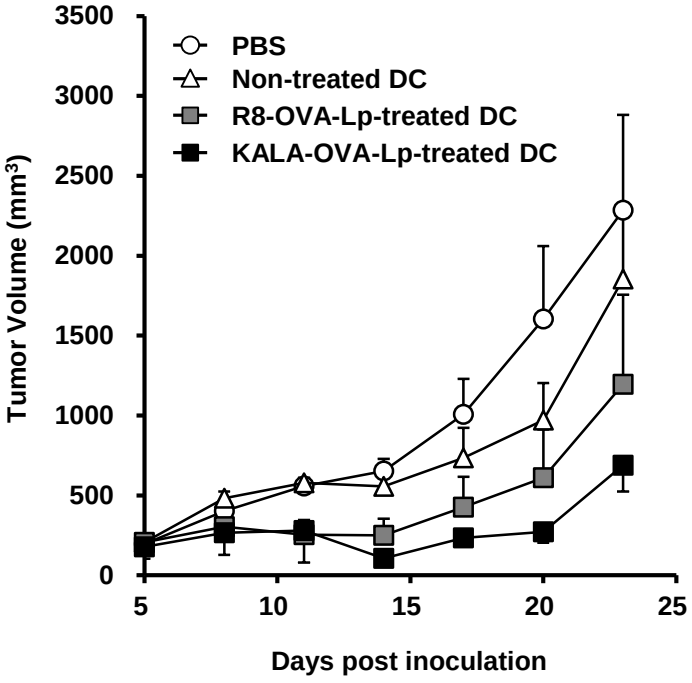

Supplementary Figure 4. *Ex vivo* anti-tumor experiment.
BMDCs (1.0×10^6 cells) were treated with the KALA-OVA-LPs or R8-OVA-LPs at a lipid dose of 32 μMd. After 6 hr incubation, the BMDCs were harvested. C57BL/6 mice were immunized with 5.0×10^5 cells of the harvested BMDCs treated with the KALA-OVA-LPs or the R8-OVA-LPs or non-treated BMDCs. At one week after immunization, mice were inoculated with 8.0×10^5 cells of E.G7-OVA in the left flank. Tumor volume was measured up to 23 days after inoculation. The plots represent the mean ± SEM (n = 4-5).

Supplementary figure 5.

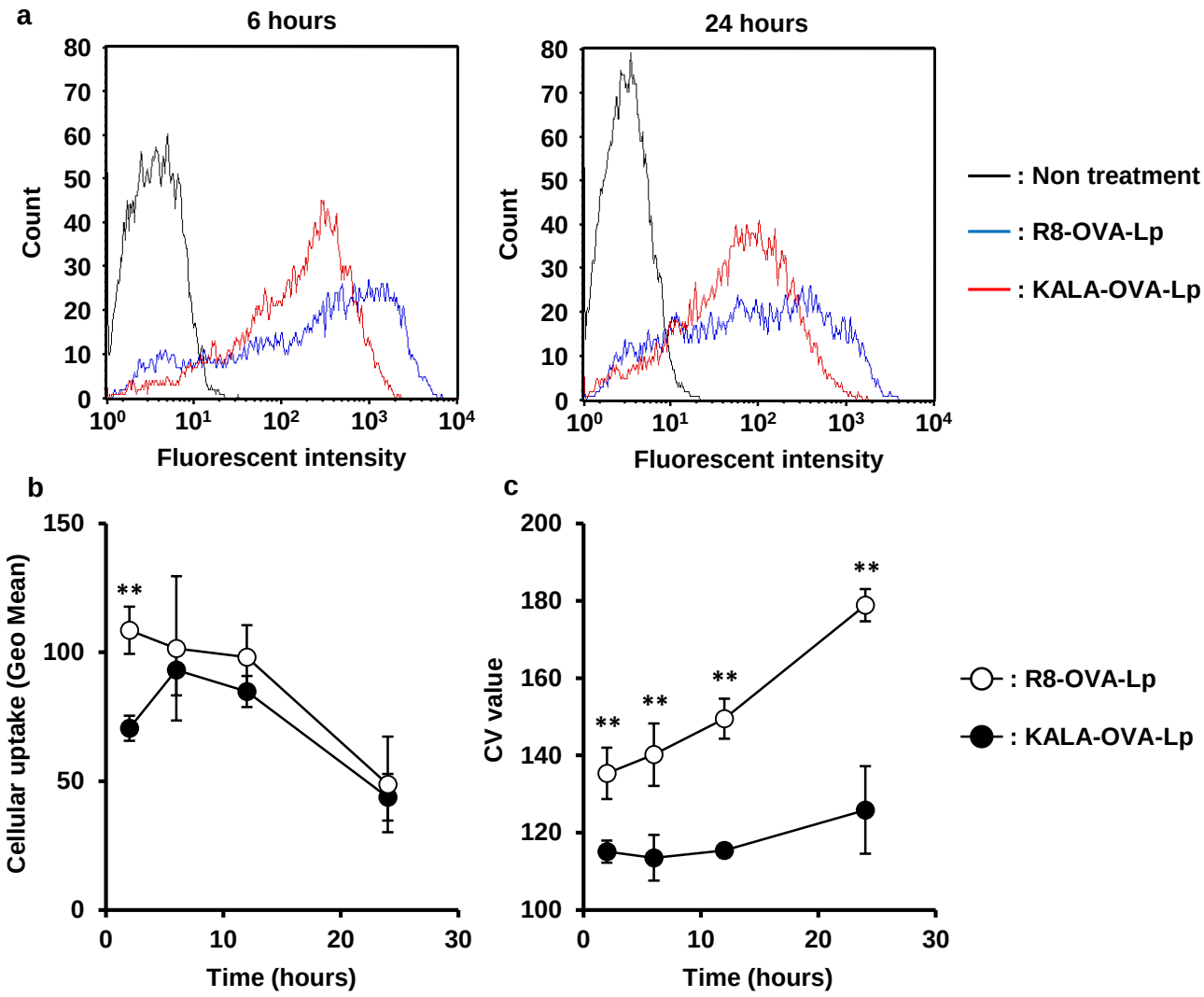

Supplementary figure 5. Uptake of KALA-OVA-LPs and R8-OVA-LPs in BMDCs.
BMDCs were treated with KALA-OVA-LPs or R8-OVA-LPs encapsulating Alexa Flour 488-labeled OVA (25% of total OVA) at a lipid dose of 32 μM. After 2, 6, 12 or 24 hours, the BMDCs were recovered and measured the fluorescent intensity by flowcytometer. (a) Typical histogram of BMDCs treated with KALA-OVA-LPs or R8-OVA-LPs. (b) Average of fluorescence intensity (Geo mean, left) and coefficient variance (CV) value (right). Data are mean ± SD (n=3). Statistical analyses were performed by Student's t-test. **P < 0.01.

Supplementary figure 6.

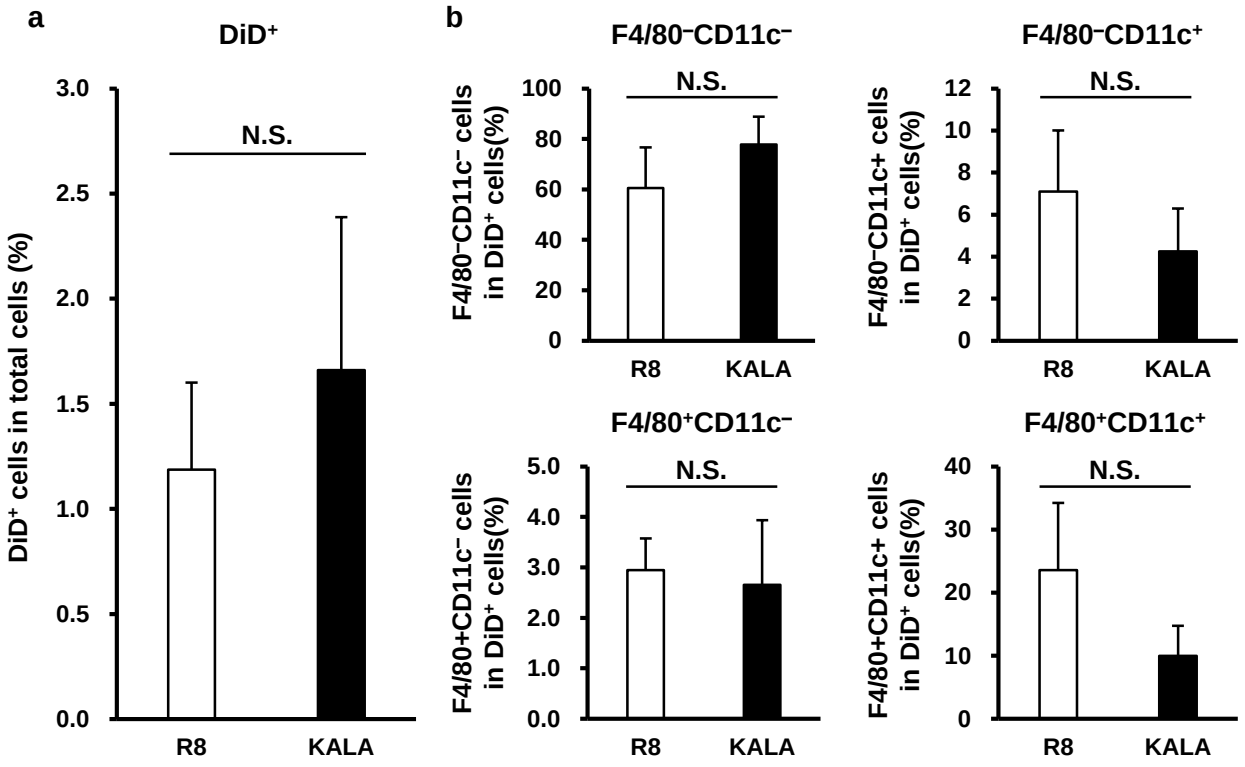

Supplementary figure 6. Lymph node accumulation of KALA-OVA-LPs and R8-OBA-LPs
C57BL/6 mice were administered subcutaneously with KALA-OVA-LPs, R8-OVA-LP modified with 0.1 mol% DiD at a dose of 25 μg OVA in the both side flanks. After 24 hours, the draining lymph nodes (inguinal lymph nodes) were isolated and mashed. Nylon mesh-filtered cell suspension were analyzed by flow cytometry for uptake of the fluorescently-labeled liposomes and expression of F4/80 and CD11c. Data are mean + SEM (n=3). Statistical analyses were performed by Student's t-test. N.S.: Not significant.